



Direct CP Violating Asymmetries in Charmless Decays of Strange Bottom Mesons and Bottom Baryons with 9.3 fb^{-1} .

The CDF Collaboration
URL <http://www-cdf.fnal.gov>
(Dated: July 12, 2012)

We report measurements of direct CP -violating asymmetries in charmless decays of neutral bottom hadrons to pairs of charged hadrons with the upgraded Collider Detector at the Fermilab Tevatron. Using a data sample corresponding to 9.3 fb^{-1} of integrated luminosity, we measure the direct CP violation in bottom strange mesons with 3.0σ significance, $A_{CP}(B_s^0 \rightarrow K^-\pi^+) = +0.22 \pm 0.07 \text{ (stat)} \pm 0.02 \text{ (syst)}$. No significant asymmetry is observed for bottom baryons where we find $A_{CP}(\Lambda_b^0 \rightarrow p\pi^-) = +0.07 \pm 0.07 \text{ (stat)} \pm 0.03 \text{ (syst)}$ and $A_{CP}(\Lambda_b^0 \rightarrow pK^-) = -0.09 \pm 0.08 \text{ (stat)} \pm 0.04 \text{ (syst)}$. In addition, we measure CP violation in $B^0 \rightarrow K^+\pi^-$ decays with 6.4σ significance, $A_{CP}(B^0 \rightarrow K^+\pi^-) = -0.083 \pm 0.013 \text{ (stat)} \pm 0.003 \text{ (syst)}$, in agreement with the current world average.

Preliminary Results for ICHEP 2012 (Summer Conferences)

I. INTRODUCTION

Non invariance of the fundamental interactions under the combined symmetry transformation of charge conjugation and parity inversion (CP violation) is an established experimental fact. The vast majority of experimental data are well described by the standard model (SM), and have supported the success of the Cabibbo-Kobayashi-Maskawa (CKM) [1] theory of quark-flavor dynamics. However, additional sources of CP violation are required to explain the matter–anti-matter asymmetry of the Universe in standard big-bang cosmology. This would have profound consequences on our understanding of fundamental interactions.

Violation of CP is *direct* if the partial decay-width (Γ) of a particle into a final state differs from the width of the corresponding antiparticle into the CP -conjugate final state. In recent times, the pattern of direct CP violation in charmless mesonic decays of B mesons has shown some unanticipated discrepancies from expectations. Under standard assumptions of isospin symmetry and smallness of contributions from higher-order processes, similar CP asymmetries are predicted for $B^0 \rightarrow K^+\pi^-$ and $B^+ \rightarrow K^+\pi^0$ decays [2, 3]. However, experimental data show a significant discrepancy [4], which has prompted intense experimental and theoretical activity. Several simple extensions of the standard model could accommodate the discrepancy [5], but uncertainty on the contribution of higher-order SM amplitudes has prevented a firm conclusion [6, 7]. High precision measurements of the violation of CP symmetry in charmless modes remains, therefore, a very interesting subject of study and may provide useful information to our comprehension of this discrepancy. Rich samples of bottom-flavored hadrons of all types from the Tevatron offer the opportunity to explore new territory in the field of B_s^0 mesons and b -flavored baryons. Additional information coming from different decays yields further constraints on the possible explanations of previous findings, and may possibly reveal new deviations from expectations.

Specifically, measurements of direct CP violation in $B_s^0 \rightarrow K^-\pi^+$ decays have been proposed as a nearly model-independent test for the presence of non-SM physics [8, 9]. The relationships between charged-current quark couplings in the SM predict a well-defined hierarchy between direct CP violation in $B^0 \rightarrow K^+\pi^-$ and $B_s^0 \rightarrow K^-\pi^+$ decays, yielding a significant asymmetry for the latter, of about 30%. This large effect allows easier experimental investigation and any discrepancy may indicate contributions from non-SM amplitudes.

Supplementary information could come from CP violation in bottom baryons. Interest in charmless b -baryon decays is prompted by branching fractions recently observed being larger than expected [10–12]. Asymmetries up to about 10% are predicted for $\Lambda_b^0 \rightarrow pK^-$ and $\Lambda_b^0 \rightarrow p\pi^-$ decays in the SM [11, 13], and are accessible with current CDF event samples.

In this document we report the measurements of direct CP violation in decays of bottom strange mesons and bottom baryons, performed in 9.3 fb^{-1} of $\bar{p}p$ collisions at $\sqrt{s} = 1.96 \text{ TeV}$, collected by the upgraded Collider Detector (CDF II) at the Fermilab Tevatron. These results represent an update of previous measurements based on a subsample of the current data sample [14].

II. DETECTOR

CDF II is a multipurpose magnetic spectrometer surrounded by calorimeters and muon detectors. The detector components relevant for this analysis are briefly outlined below; a more detailed description can be found in Ref. [15]. A silicon microstrip vertex detector (SVX) and a cylindrical drift chamber (COT) immersed in a 1.4 T axial magnetic field allow reconstruction of charged-particle trajectories (tracks) in the pseudorapidity range $|\eta| < 1.0$ [16]. The SVX consists of six concentric layers of double-sided silicon sensors with radii between 2.5 and 22 cm, each providing a measurement with up to 15 (70) μm resolution in the ϕ (z) direction. The COT has 96 measurement layers, between 40 and 137 cm in radius, organized into alternating axial and $\pm 2^\circ$ stereo superlayers. The transverse momentum resolution is $\sigma_{p_T}/p_T^2 \sim 0.15\% / (\text{GeV}/c)$, corresponding to a typical mass resolution of $22 \text{ MeV}/c^2$ for our signals. The specific ionization energy loss (dE/dx) of charged particles in the COT can be measured from the collected charge, which is logarithmically encoded in the output pulse width of each wire, and provides 1.4σ separation between kaons and pions with momenta greater than $2 \text{ GeV}/c$.

III. SAMPLE AND SELECTION

The data were collected by a three-level trigger system, using a set of requirements specifically aimed at selecting two-pronged B decays. At level 1, COT tracks are reconstructed in the transverse plane by a hardware processor (XFT) [17]. Two opposite-charge particles are required, with reconstructed transverse momenta $p_{T1}, p_{T2} > 2 \text{ GeV}/c$, the scalar sum $p_{T1} + p_{T2} > 5.5 \text{ GeV}/c$, and an azimuthal opening-angle $\Delta\phi < 135^\circ$. At level 2, the silicon vertex trigger (SVT) [18] combines XFT tracks with SVX hits to measure the impact parameter d (distance of closest approach to

the beam line) of each track with $45 \mu\text{m}$ resolution. The requirement of two tracks with $0.1 < d < 1.0 \text{ mm}$ reduces the light-quark background by two orders of magnitude while preserving about half of the signal. A tighter opening-angle requirement, $20^\circ < \Delta\phi < 135^\circ$, preferentially selects two-body B decays over multi-body decays with 97% efficiency and further reduces background. Each track pair is then used to form a B candidate, which is required to have an impact parameter $d_B < 140 \mu\text{m}$ and to have travelled a distance $L_T > 200 \mu\text{m}$ in the transverse plane. At level 3, an array of computers confirms the selection with a full event reconstruction. The overall acceptance of the trigger selection is $\approx 2\%$ for b -hadrons with $p_T > 4 \text{ GeV}/c$ and $|\eta| < 1$.

The offline selection is based on a more accurate determination of the same quantities used in the trigger, with the addition of two further observables: the isolation (I_B) of the B candidate [19], and the quality of the three-dimensional fit (χ^2 with 1 d.o.f.) of the decay vertex of the B candidate. Requiring a large value of I_B reduces the background from light-quark jets, and a low χ^2 reduces the background from decays of different long-lived particles within the event, owing to the good resolution of the SVX detector in the z direction. The final selection, inherited from Ref. [12], was originally devised for the $B_s^0 \rightarrow K^- \pi^+$ search, but has proven to be optimal also for measuring $A_{CP}(B_s^0 \rightarrow K^- \pi^+)$. This includes the following criteria: $I_B > 0.525$, $\chi^2 < 5$, $d > 120 \mu\text{m}$, $d_B < 60 \mu\text{m}$, and $L_T > 350 \mu\text{m}$. No more than one B candidate per event is found after this selection, and a mass $m_{\pi\pi}$ is assigned to each, using a charged pion mass assignment for both decay products. The resulting mass distribution is shown in Fig. 1. The peak is visible, dominated by the overlapping contributions of the $B^0 \rightarrow K^+ \pi^-$, $B^0 \rightarrow \pi^+ \pi^-$, and $B_s^0 \rightarrow K^+ K^-$ modes [14, 20]. The other modes $B_s^0 \rightarrow K^- \pi^+$, $\Lambda_b^0 \rightarrow p \pi^-$ and $\Lambda_b^0 \rightarrow p K^-$ [12], relevant for this measurement, appear at masses higher than the main peak ($5.33\text{--}5.55 \text{ GeV}/c^2$) on its high tail. Backgrounds include mis-reconstructed multi-body b -hadron decays (physics background) and random pairs of charged particles (combinatorial background).

IV. FIT OF COMPOSITION

We use an unbinned likelihood fit, incorporating kinematic (kin) and particle identification (PID) information, to determine the fraction of each individual mode and the charge asymmetries, uncorrected for instrumental effects, $\tilde{A}_{CP} = [N_{b \rightarrow f} - N_{\bar{b} \rightarrow \bar{f}}]/[N_{b \rightarrow f} + N_{\bar{b} \rightarrow \bar{f}}]$ of the flavor-specific decays $B^0 \rightarrow K^+ \pi^-$, $B_s^0 \rightarrow K^- \pi^+$, and $\Lambda_b^0 \rightarrow p \pi^-$, $p K^-$. For each channel, $N_{b \rightarrow f}$ ($N_{\bar{b} \rightarrow \bar{f}}$) is the reconstructed number of decays of hadrons containing the b (\bar{b}) quark into the final state f (\bar{f}). The decay flavor is inferred from the charges of final state particles assuming equal numbers of b and \bar{b} quarks at production (dominated by the strong interaction). Any effect from CP violation in b -meson flavor mixing is assumed negligible [21]. The likelihood for the i th event is

$$\begin{aligned} \mathcal{L}_i = & (1 - b) \sum_j f_j \mathcal{L}_j^{\text{kin}} \mathcal{L}_j^{\text{PID}} \\ & + b (f_p \mathcal{L}_p^{\text{kin}} \mathcal{L}_p^{\text{PID}} + (1 - f_p) \mathcal{L}_c^{\text{kin}} \mathcal{L}_c^{\text{PID}}), \end{aligned} \quad (1)$$

where the index j runs over all signal modes, and the index ‘p’ (‘c’) labels the physics (combinatorial) background terms. The f_j are the signal fractions to be determined by the fit, together with the background fraction parameters b and f_p .

The kinematic information is summarized by three loosely correlated observables: (a) the square mass $m_{\pi\pi}^2$; (b) the charged momentum asymmetry $\beta = (p_+ - p_-)/(p_+ + p_-)$, where p_+ (p_-) is the momentum of the positive(negative) particle; (c) the scalar sum of particle momenta $p_{\text{tot}} = p_+ + p_-$. The above variables allow evaluation of the square invariant mass m_{+-}^2 of a candidate for any mass assignment of the positive and negative decay products (m_+, m_-), using the equation

$$\begin{aligned} m_{+-}^2 = & m_{\pi\pi}^2 - 2m_\pi^2 + m_+^2 + m_-^2 + \\ & -2\sqrt{p_+^2 + m_\pi^2} \sqrt{p_-^2 + m_\pi^2} + 2\sqrt{p_+^2 + m_+^2} \sqrt{p_-^2 + m_-^2}, \end{aligned} \quad (2)$$

where $p_+ = p_{\text{tot}} \frac{1+\beta}{2}$, $p_- = p_{\text{tot}} \frac{1-\beta}{2}$.

We used data to obtain the kinematic distributions of combinatorial background [22] and simulation for physics backgrounds. The square mass distribution of the combinatorial background is parameterized by an exponential function. The slope is fixed in the fit and it has been extracted from an enriched sample of two generic random tracks, containing events that pass the final selections except for the requirement on the vertex quality, which is inverted to $\chi^2 > 40$. The physics background is modeled by an empirical threshold function, defined as $x \cdot \sqrt{1 - (x/x_0)^2}$ if $x < x_0$ (where $x = m_{\pi\pi}^2$), convoluted with a Gaussian resolution function. The cutoff x_0 is a fixed parameter in the fit, and its value is $26.64 \text{ GeV}^2/c^4$. This has been determined as the minimum value of the $-2 \log \mathcal{L}$ profile obtained repeating the fit spanning the cutoff value (fixed in the fit) in the range $[26.4, 26.8] \text{ GeV}^2/c^4$ with a step of 0.001

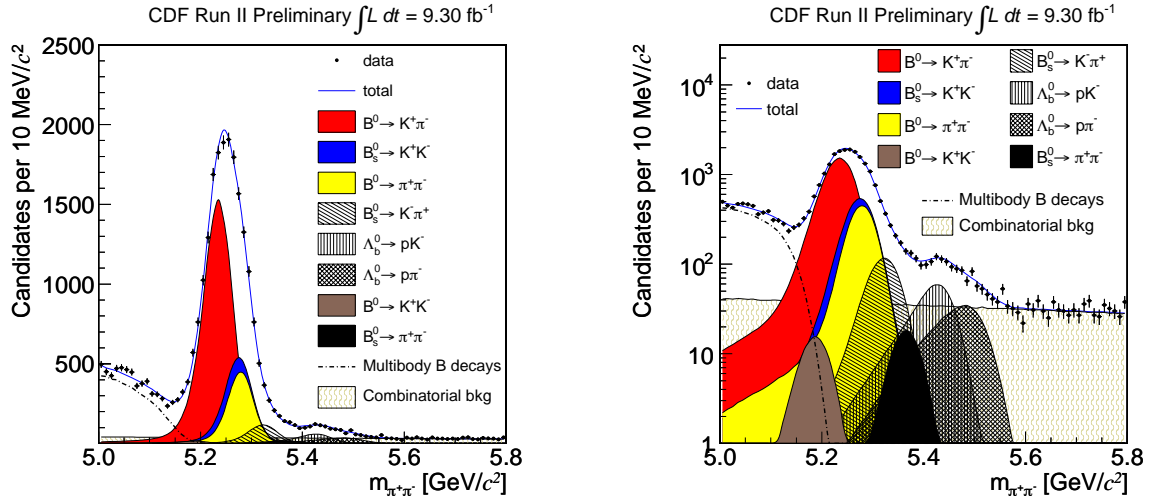


FIG. 1: Mass distribution of reconstructed candidates, $m_{\pi\pi}$. The charged pion mass is assigned to both tracks. The total projection is overlaid on the data distribution.

GeV^2/c^4 . A systematic uncertainty is assessed on the observables of interest taking the difference between the central fit (minimum of the profile) and the fits intersecting the horizontal line at $-2\Delta \log \mathcal{L} = 4$, corresponding to a 95%CL interval.

In order to ensure the reliability of the search for small signals in the vicinity of larger peaks, the shapes of the mass distributions assigned to each signal have been modeled in detail. The momentum dependence and non-Gaussian tails of resolution are included from a full simulation of the detector, while the effects of soft photon radiation in the final state are based on PHOTOS package [23]. This resolution model was checked against the observed shape of the $3.8 \times 10^6 D^0 \rightarrow K^- \pi^+$ decays in a sample of $D^{*+} \rightarrow D^0 \pi^+$ decays, collected with a similar trigger selection. The $D^{*+} \rightarrow D^0 \pi^+$ sample was also used to calibrate the dE/dx response of the drift chamber to kaons and pions, using the charge of the D^{*+} pion to identify the D^0 decay products. The dE/dx response of protons was determined from a sample of about $3.3 \times 10^5 \Lambda \rightarrow p \pi^-$ decays, where the kinematics and the momentum threshold of the trigger allow unambiguous identification of the decay products [24]. PID information is summarized by a single observable kaonness, defined as:

$$\kappa = \frac{dE/dx - dE/dx(\pi)}{dE/dx(K) - dE/dx(\pi)} \quad (3)$$

where $dE/dx(\pi)$ and $dE/dx(K)$ are the expected dE/dx depositions for those particle assignments. The average values of κ expected for pions and kaons are by construction 0 and 1. Statistical separation between kaons and pions is about 1.4σ , while the ionization rates of protons and kaons are quite similar in the momentum range of interest. The PID likelihood term, which is similar for physics signals and backgrounds, depends only on the kaonness and on the expected kaonness (given a mass hypothesis) of the decay products. In particular the physics signals model is described by the likelihood term $\mathcal{L}_j^{\text{PID}}$, where the index j defines the particles in the final state, while the background model is described by the two terms $\mathcal{L}_p^{\text{PID}}$ and $\mathcal{L}_c^{\text{PID}}$, respectively for the physics and combinatorial background, that account for all possible pairs that can be formed combining only pions and kaons. In fact muons are indistinguishable from pions with the available dE/dx resolution, and are therefore included within the nominal pion component. For similar reasons, the small proton component in the background has been included within the nominal kaon component. Thus the physics background model allows for independent, charge-averaged contributions of pions and kaons, whose fractions are determined by the fit; while the combinatorial background model, instead, allows for more contributions, since independent fractions of positively and negatively charged pions and kaons are determined by the fit.

Figures 1-2 show the distributions of the discriminant observables with fit projections overlaid.

Figure 3 demonstrates how kinematic and PID information enables the separation of signal modes, especially for CP -conjugated final states.

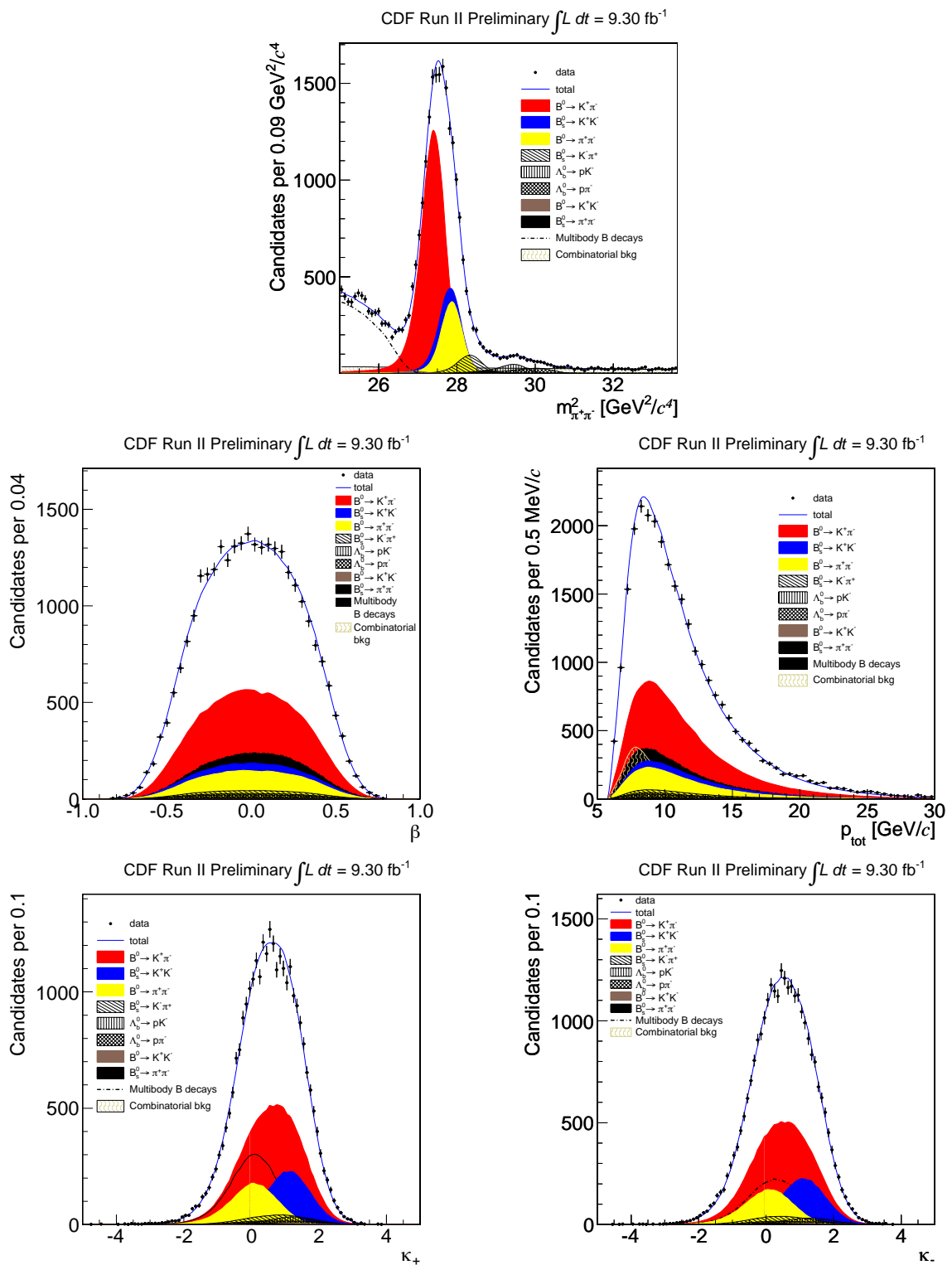


FIG. 2: $m_{\pi\pi}^2$, β , p_{tot} , κ_+ and κ_- distribution of reconstructed candidates. The total projection is overlaid on the data distribution.

V. FIT RESULTS

The signal yields from the fit (Table I) are corrected for different detection efficiencies to determine the physical asymmetries $A_{CP}(b \rightarrow f)$, defined as

$$\frac{\mathcal{B}(b \rightarrow f) - \mathcal{B}(\bar{b} \rightarrow \bar{f})}{\mathcal{B}(b \rightarrow f) + \mathcal{B}(\bar{b} \rightarrow \bar{f})} = \frac{N_{b \rightarrow f} - c_f N_{\bar{b} \rightarrow \bar{f}}}{N_{b \rightarrow f} + c_f N_{\bar{b} \rightarrow \bar{f}}}, \quad (4)$$

where $c_f = \varepsilon(f)/\varepsilon(\bar{f})$ is the ratio between the efficiencies for triggering and reconstructing the final state f with respect to the state \bar{f} . The c_f factors correct for detector-induced charge asymmetries, and are extracted from control samples in data. Simulation is used only to account for small differences between the kinematics of $B \rightarrow h^+ h'^-$ decays and control signals. The corrections for $f = K^+ \pi^-$ are extracted from a sample of about 30×10^6 untagged $D^0 \rightarrow K^- \pi^+$ decays, corresponding to an integrated luminosity of about 6 fb^{-1} . By imposing the same offline selection to the D^0 decays, we obtain $K^\mp \pi^\pm$ final states in a similar kinematic region as our signals. We assume that $K^+ \pi^-$ and $K^- \pi^+$ final states from charm decays are produced in equal numbers at the Tevatron, because production is dominated by the strong interaction and, compared to the detector effects to be corrected, the possible CP -violating asymmetry in $D^0 \rightarrow K^- \pi^+$ decays is tiny ($< 10^{-3}$) as predicted by the SM [25] and confirmed by current experimental determinations [26]. We also checked that possible asymmetries in D^0 meson yields induced by CP violation in $B \rightarrow DX$ decays are small and can be neglected [27]. Therefore, any asymmetry between observed numbers of reconstructed $K^- \pi^+$ and $K^+ \pi^-$ charm decays can be ascribed to detector-induced effects and used to extract the desired correction factors. The ratio $N_{\bar{D}^0 \rightarrow K^+ \pi^-} / N_{D^0 \rightarrow K^- \pi^+}$ is measured performing a simultaneous fit described in [27]. The dE/dx information is not used because kinematics alone is sufficient to provide an excellent separation in charm decays, as shown in Ref. [27]. We find $c_{K^- \pi^+} = 0.983 \pm 0.001$, which is consistent and more precise than a previous estimate done at CDF [24]. For the $\Lambda_b^0 \rightarrow p \pi^-$ asymmetry, the factor $c_{p \pi^-} = 1.01 \pm 0.02$ is extracted using a similar strategy applied to a control sample of $\Lambda \rightarrow p \pi$ decays [22]. This correction is extracted from a simultaneous fit evaluating the yields of $\Lambda \rightarrow p \pi^+$ and of $\bar{\Lambda} \rightarrow \bar{p} \pi^-$ and is dominated by the different interaction probability of protons and antiprotons with the detector material. In the measurement of CP violation in $\Lambda_b^0 \rightarrow p K^-$ decays, instrumental charge-asymmetries induced in both kaons and protons are relevant. The $c_{p K^-}$ factor is extracted by combining the previous ones and assuming the trigger and reconstruction efficiency for two particles factorizes as the product of the single-particle efficiencies.

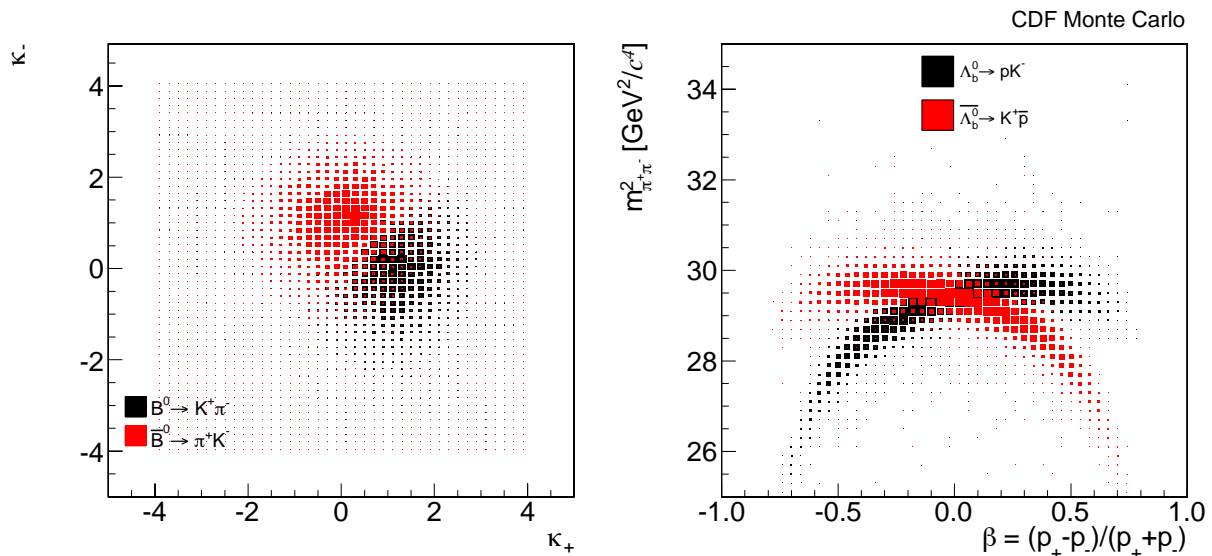


FIG. 3: Joint kaonness distribution for the positive (abscissa) and negative (ordinate) final state particles in $B^0 \rightarrow K^+ \pi^-$ decays as determined from the calibration data of charm decays (left panel). Dipion mass as a function of β for simulated $\Lambda_b^0 \rightarrow p K^-$ decays (right panel).

TABLE I: Direct CP asymmetries. The first quoted uncertainty is statistical, the second is systematic. \mathcal{N} is the number of fitted events for each mode.

Mode	\mathcal{N}	Quantity	Measurement
$B^0 \rightarrow K^+\pi^-$	6348 ± 117	$\frac{\mathcal{B}(\overline{B}^0 \rightarrow K^-\pi^+) - \mathcal{B}(B^0 \rightarrow K^+\pi^-)}{\mathcal{B}(\overline{B}^0 \rightarrow K^-\pi^+) + \mathcal{B}(B^0 \rightarrow K^+\pi^-)}$	$-0.083 \pm 0.013 \pm 0.003$
$\overline{B}^0 \rightarrow K^-\pi^+$	5313 ± 109		
$B_s^0 \rightarrow K^-\pi^+$	354 ± 46	$\frac{\mathcal{B}(\overline{B}_s^0 \rightarrow K^+\pi^-) - \mathcal{B}(B_s^0 \rightarrow K^-\pi^+)}{\mathcal{B}(\overline{B}_s^0 \rightarrow K^+\pi^-) + \mathcal{B}(B_s^0 \rightarrow K^-\pi^+)}$	$+0.22 \pm 0.07 \pm 0.02$
$\overline{B}_s^0 \rightarrow K^+\pi^-$	560 ± 51		
$\Lambda_b^0 \rightarrow p\pi^-$	242 ± 24	$\frac{\mathcal{B}(\Lambda_b^0 \rightarrow p\pi^-) - \mathcal{B}(\overline{\Lambda}_b^0 \rightarrow \overline{p}\pi^+)}{\mathcal{B}(\Lambda_b^0 \rightarrow p\pi^-) + \mathcal{B}(\overline{\Lambda}_b^0 \rightarrow \overline{p}\pi^+)}$	$+0.07 \pm 0.07 \pm 0.03$
$\overline{\Lambda}_b^0 \rightarrow \overline{p}\pi^+$	206 ± 23		
$\Lambda_b^0 \rightarrow pK^-$	271 ± 30	$\frac{\mathcal{B}(\Lambda_b^0 \rightarrow pK^-) - \mathcal{B}(\overline{\Lambda}_b^0 \rightarrow \overline{p}K^+)}{\mathcal{B}(\Lambda_b^0 \rightarrow pK^-) + \mathcal{B}(\overline{\Lambda}_b^0 \rightarrow \overline{p}K^+)}$	$-0.09 \pm 0.08 \pm 0.04$
$\overline{\Lambda}_b^0 \rightarrow \overline{p}K^+$	324 ± 31		

VI. SYSTEMATICS

A synopsis of all the systematic uncertainties is reported in Table II. The total systematic uncertainty on each measurement has been determined as the sum in quadrature of the single systematic uncertainties. When the systematic uncertainty is asymmetric, the larger value has been used in the squared sum.

TABLE II: Summary of the systematic uncertainties.

source	$A_{CP}(B^0 \rightarrow K^+\pi^-)$	$A_{CP}(B_s^0 \rightarrow K^-\pi^+)$	$A_{CP}(\Lambda_b^0 \rightarrow p\pi^-)$	$A_{CP}(\Lambda_b^0 \rightarrow pK^-)$
Charge asymm. of momentum p.d.f	0.0011	0.0025	0.0009	0.0022
Signals momentum p.d.f.	0.0013	0.0043	0.0054	0.0103
Combinatorial back. momentum p.d.f	0.0004	0.0072	0.0257	0.0065
Physics back. momentum p.d.f	0.0008	0.0002	0.0003	0.0004
Signals mass p.d.f.	0.0002	0.0066	0.0018	0.0006
Combinatorial back. mass p.d.f.	<0.0001	0.0001	<0.0001	<0.0001
Physics back. mass p.d.f	0.0001	0.0006	0.0005	0.0001
Particle Identification model	0.0023	0.0066	0.0040	0.0046
Charge asymmetry	0.0014	0.0013	0.0094	0.0096
Triggers relative efficiency	0.0003	0.0083	0.0004	0.0034
Nominal b -hadrons masses	0.0001	0.0049	0.0007	0.0008
$p_T(\Lambda_b^0)$ spectrum	0.0001	0.0010	0.0052	0.0021
Λ_b^0 polarization	<0.0001	0.0027	0.0089	0.0364
TOTAL	0.003	0.02	0.03	0.04

VII. FINAL COMMENTS

The final results are listed in Table I. We report an updated measurement of $A_{CP}(B^0 \rightarrow K^+\pi^-)$ with a significance more than 5σ . The uncertainty of the observed asymmetry is consistent and of comparable accuracy with current

results from asymmetric e^+e^- colliders [4] and LHCb [28]. We report an updated measurement of $A_{CP}(B_s^0 \rightarrow K^-\pi^+)$ with a significance of 2.9σ . This result confirms the LHCb evidence [28] with the same level of resolution. The averaged value between this result and LHCb measurement is equal to $A_{CP}(B_s^0 \rightarrow K^-\pi^+)_{\text{mean}} = +0.242 \pm 0.054$ which has a significance of 4.5σ . This represents a strong evidence of CP violation in the B_s^0 mesons system. The observed asymmetry in the $\Lambda_b^0 \rightarrow pK^-$ decays and in the $\Lambda_b^0 \rightarrow p\pi^-$ decays are consistent with zero. However, the limited experimental precision does not allow a conclusive discrimination between the standard model prediction (8%) and much suppressed values ($\approx 0.3\%$) expected in R-parity violating supersymmetric scenarios [13]. The observed asymmetries are consistent with the previous results from CDF in Ref. [14] and supersedes them.

In summary, we have measured the CP asymmetries of charmless neutral b -mesons and baryons into pairs of charged mesons in CDF data. We report the updated measurements of $A_{CP}(B^0 \rightarrow K^+\pi^-)$, $A_{CP}(B_s^0 \rightarrow K^-\pi^+)$, $A_{CP}(\Lambda_b^0 \rightarrow p\pi^-)$ and $A_{CP}(\Lambda_b^0 \rightarrow pK^-)$.

Acknowledgments

We thank the Fermilab staff and the technical staffs of the participating institutions for their vital contributions. This work was supported by the U.S. Department of Energy and National Science Foundation; the Italian Istituto Nazionale di Fisica Nucleare; the Ministry of Education, Culture, Sports, Science and Technology of Japan; the Natural Sciences and Engineering Research Council of Canada; the National Science Council of the Republic of China; the Swiss National Science Foundation; the A.P. Sloan Foundation; the Bundesministerium für Bildung und Forschung, Germany; the Korean World Class University Program, the National Research Foundation of Korea; the Science and Technology Facilities Council and the Royal Society, UK; the Institut National de Physique Nucleaire et Physique des Particules/CNRS; the Russian Foundation for Basic Research; the Ministerio de Ciencia e Innovación, and Programa Consolider-Ingenio 2010, Spain; the Slovak R&D Agency; and the Academy of Finland.

-
- [1] M. Kobayashi and T. Maskawa, Prog. Theor. Phys. **49**, 652 (1973).
 - [2] Y.Y. Keum and A.I. Sanda, Phys. Rev. D **67**, 054009 (2003).
 - [3] M. Beneke and M. Neubert, Nucl. Phys. **B675**, 333 (2003);
 - [4] S.-W. Lin *et al.* (Belle Collaboration), Nature **452**, 332 (2008); B. Aubert *et al.* (BABAR Collaboration), Phys. Rev. Lett. **99**, 021603 (2007); B. Aubert *et al.* (BABAR Collaboration), Phys. Rev. D **76**, 091102 (2007).
 - [5] See for instance W.-S. Hou, M. Nagashima, and A. Soddu, Phys. Rev. Lett. **95**, 141601 (2005) or S. Baek *et al.*, Phys. Rev. D **71**, 057502 (2005).
 - [6] H.-S. Li, S. Mishima, and A.I. Sanda, Phys. Rev. D **72**, 114005 (2005).
 - [7] H. J. Lipkin, arXiv:1105.3443 [hep-ph].
 - [8] M. Gronau and J. L. Rosner, Phys. Lett. B **482**, 71 (2000).
 - [9] H. J. Lipkin, Phys. Lett. B **621**, 126 (2005).
 - [10] R. Mohanta, A. K. Giri, and M. P. Khanna, Phys. Rev. D **63**, 074001 (2001).
 - [11] C.-D. Lu *et al.*, Phys. Rev. D **80**, 034011 (2009).
 - [12] T. Aaltonen *et al.* (CDF Collaboration), Phys. Rev. Lett. **103**, 031801 (2009).
 - [13] R. Mohanta, Phys. Rev. D **63**, 056006 (2001).
 - [14] A. Aaltonen *et al.* (CDF Collaboration), Phys. Rev. Lett. **106**, 181802 (2011).
 - [15] D. Acosta *et al.* (CDF Collaboration), Phys. Rev. D **71**, 032001 (2005);
 - [16] CDF II uses a cylindrical coordinate system in which ϕ is the azimuthal angle, r is the radius from the nominal beam line, and z points in the proton beam direction, with the origin at the center of the detector. The transverse plane is the plane perpendicular to the z axis.
 - [17] E. Thomson *et al.*, IEEE Trans. Nucl. Sci. **49**, 1063 (2002); R. Downing *et al.*, Nucl. Instrum. Methods A **570**, 36 (2007).
 - [18] B. Ashmanskas *et al.*, Nucl. Instrum. Methods A **518**, 532 (2004).
 - [19] Isolation is defined as $I_B = p_T(B)/(p_T(B) + \sum_i p_{Ti})$, where $p_T(B)$ is the transverse momentum of the B candidate, and the sum runs over all other tracks within a cone of radius 1, in η - ϕ space around the B flight-direction.
 - [20] A. Abulencia *et al.* (CDF Collaboration), Phys. Rev. Lett. **97**, 211802 (2006).
 - [21] K. Nakamura *et al.*, J. Phys. G **37**, 075021 (2010).
 - [22] F. Ruffini, Ph.D. Thesis, Università di Siena, Siena, in preparation.
 - [23] E. Barberio and Z. Was, Comput. Phys. Commun. **79**, 291 (1994).
 - [24] M.J. Morello, Ph.D. Thesis, Scuola Normale Superiore, Pisa, Fermilab Report No. FERMILAB-THESIS-2007-57 (2007).
 - [25] S. Bianco, F. L. Fabbri, D. Benson, and I. Bigi, Riv. Nuovo Cimento **26N7**, 1 (2003).
 - [26] B. Aubert *et al.* (BABAR Collaboration), Phys. Rev. Lett. **100**, 061803 (2008); M. Starič *et al.* (Belle Collaboration), Phys. Lett. B **670**, 190 (2008).
 - [27] T. Aaltonen *et al.* (CDF Collaboration), Phys. Rev. D **85**, 012009 (2012).

- [28] R. Aaij *et al.* [LHCb Collaboration], Phys. Rev. Lett. **108** (2012) 201601 [arXiv:1202.6251 [hep-ex]].